

# Electrophysiological Characterization of the Human Na<sup>+</sup>/Nucleoside Cotransporter 1 (hCNT1) and Role of Adenosine on hCNT1 Function\*

Received for publication, October 31, 2003, and in revised form, December 19, 2003  
Published, JBC Papers in Press, December 29, 2003, DOI 10.1074/jbc.M311940200

Ignacio M. Larráyoza‡§, Francisco Javier Casado¶, Marçal Pastor-Anglada¶, and M. Pilar Lostao‡¶

From the ‡Departamento de Fisiología y Nutrición, Universidad de Navarra, Pamplona 31080, Spain and ¶Departament de Bioquímica i Biologia Molecular, Facultat de Biologia, Universitat de Barcelona, Barcelona E-08071, Spain

We previously reported that the human Na<sup>+</sup>/nucleoside transporter pyrimidine-preferring 1 (hCNT1) is electrogenic and transports gemcitabine and 5'-deoxy-5-fluorouridine, a precursor of the active drug 5-fluorouracil. Nevertheless, a complete electrophysiological characterization of the basic properties of hCNT1-mediated translocation has not been performed yet, and the exact role of adenosine in hCNT1 function has not been addressed either. In the present work we have used the two-electrode voltage clamp technique to investigate hCNT1 transport mechanism and study the kinetic properties of adenosine as an inhibitor of hCNT1. We show that hCNT1 exhibits presteady-state currents that disappear upon the addition of adenosine or uridine. Adenosine, a purine nucleoside described as a substrate of the pyrimidine-preferring transporters, is not a substrate of hCNT1 but a high affinity blocker able to inhibit uridine-induced inward currents, the Na<sup>+</sup>-leak currents, and the presteady-state currents, with a *K<sub>i</sub>* of 6.5 μM. The kinetic parameters for uridine, gemcitabine, and 5'-deoxy-5-fluorouridine were studied as a function of membrane potential; at -50 mV, *K<sub>0.5</sub>* was 37, 18, and 245 μM, respectively, and remained voltage-independent. *I<sub>max</sub>* for gemcitabine was voltage-independent and accounts for ~40% that for uridine at -50 mV. Maximal current for 5'-DFUR was voltage-dependent and was ~150% that for uridine at all membrane potentials. *K<sub>0.5</sub><sup>Na+</sup>* for Na<sup>+</sup> was voltage-independent at hyperpolarized membrane potentials (1.2 mM at -50 mV), whereas *I<sub>max</sub><sup>Na+</sup>* was voltage-dependent, increasing 2-fold from -50 to -150 mV. Direct measurements of <sup>3</sup>H-nucleoside or <sup>22</sup>Na fluxes with the charge-associated revealed a ratio of two positive inward charges per nucleoside and one Na<sup>+</sup> per positive inward charge, suggesting a stoichiometry of two Na<sup>+</sup>/nucleoside.

Nucleoside uptake into cells occurs through specific transport proteins located at the plasma membrane. These transporters belong to two families of integral membrane proteins,

the equilibrative nucleoside transporter family or ENT, with broad substrate selectivity, and the concentrative nucleoside transporter family or CNT<sup>1</sup> (1–4). The CNT transporters are Na<sup>+</sup>-dependent, and they differ in substrate selectivity. Among them, three CNT isoforms have been cloned so far; they are CNT1, which is pyrimidine-preferring, CNT2, which is purine-preferring (2–4), and CNT3, which shows broad selectivity, accepting both pyrimidine and purine nucleosides (5). Besides the important function of nucleosides as precursors of nucleic acid and energy-rich molecules, a variety of nucleoside-derived drugs used in cancer and anti-viral therapies are taken up by the cells through the nucleoside transporters (2, 3, 6, 7).

Although the electrogenic property of CNT transporters has been used to study their substrate selectivity at a fixed membrane potential (5–12), the electrophysiological characteristics of the transport mechanism are not known. Therefore, the detailed electrophysiological analysis of hCNT1-mediated substrate translocation and inhibitor interaction will be helpful in the understanding of the minimal structural requirements of substrates and inhibitors, thus contributing to improve therapeutics using hCNT1 as a pharmacological target.

We previously reported that the human Na<sup>+</sup>/nucleoside transporter pyrimidine-preferring 1 (hCNT1) is electrogenic (6, 7). In the present work we have used electrophysiological methods to characterize hCNT1 and show the presteady-state currents, directly determine the Na<sup>+</sup>-nucleoside stoichiometry, and study the kinetic properties of natural nucleosides and relevant nucleoside-derived drugs. A major finding of this contribution is also the unequivocal demonstration that adenosine is not a hCNT1 substrate but can efficiently block the uptake of pyrimidine nucleosides. Although the impact of this inhibition in physiology and pharmacology still has to be elucidated, this finding anticipates new physiological roles for adenosine besides its well known actions as purinergic agonist.

## EXPERIMENTAL PROCEDURES

*Expression of hCNT1 in Xenopus laevis Oocytes and Uptake Assays*—Stage VI oocytes from *X. laevis* (Blades Biological, Cowden, UK) were obtained as previously described (13). They were microinjected with 30–50 ng of mRNA coding for the human Na<sup>+</sup>/nucleoside cotransporter 1, hCNT1 (6), and were maintained at 18 °C in Barth's medium (88 mM NaCl, 1 mM KCl, 0.33 mM Ca(NO<sub>3</sub>)<sub>2</sub>, 0.41 mM CaCl<sub>2</sub>, 0.82 mM MgSO<sub>4</sub>, 2.4 mM NaHCO<sub>3</sub> and 10 mM HEPES-Tris, pH 7.4) containing gentamycin (50 mg/liter) and chloramphenicol (1 mg/ml). Experiments were performed at 22 ± 1 °C 2–7 days after the injection.

Nucleoside uptake was measured by a radiotracer method (14). Briefly, groups of 6–10 oocytes were incubated for 1 h in 400 μl of Na<sup>+</sup> buffer solution (100 mM NaCl, 2 mM KCl, 1 mM MgCl<sub>2</sub>, 1 mM CaCl<sub>2</sub>, and

\* This work has been supported by the Plan de Investigación Universidad de Navarra, Departamento de Educación de la Navarra Government and Ministerio de Ciencia y Tecnología (Spanish Government) Grants BF12003-01371 (to M. P. L.) and SAF2002-0717 (to M. P.-A.). The costs of publication of this article were defrayed in part by the payment of page charges. This article must therefore be hereby marked "advertisement" in accordance with 18 U.S.C. Section 1734 solely to indicate this fact.

§ A fellow of the Asociación de Amigos (University of Navarra).

¶ To whom correspondence may be addressed: Departamento de Fisiología y Nutrición, Universidad de Navarra, c/Irunlarrea s/n, Pamplona 31080, Spain. Tel.: 948-42-56-00; Fax: 948-42-56-49; E-mail: plostao@unav.es.

<sup>1</sup> The abbreviations used are: CNT, concentrative nucleoside transporter; 5'-DFUR, 5'-deoxy-5-fluorouridine; gemcitabine, 2'-2'-difluoro-deoxy-cytidine.

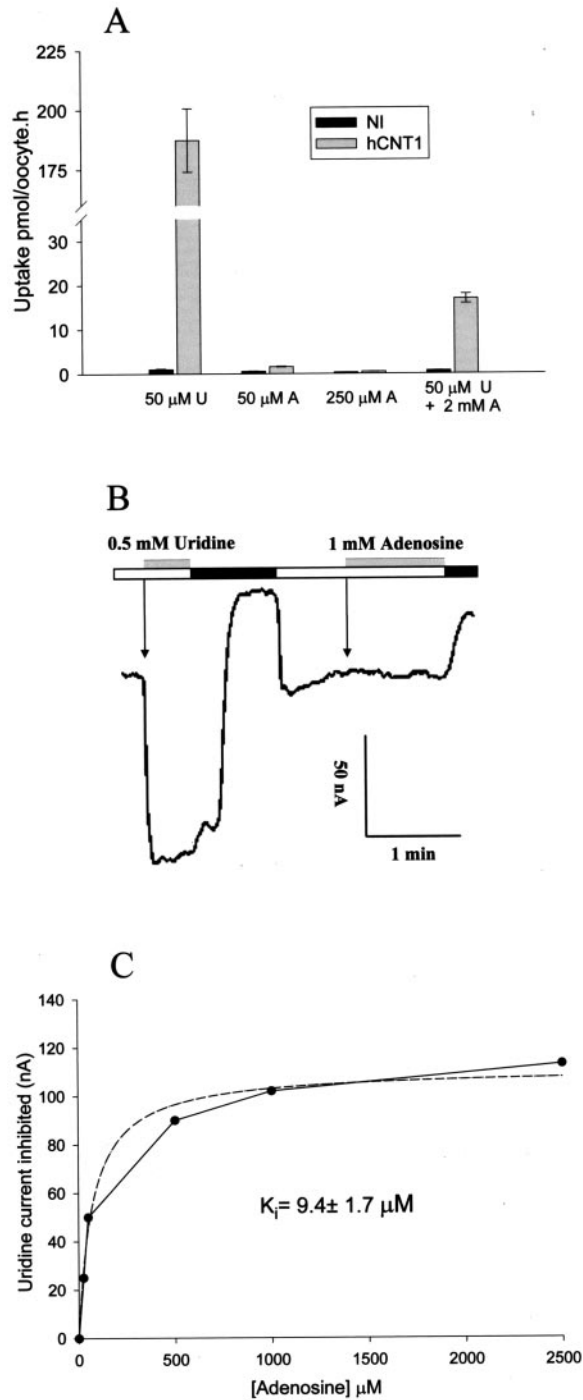


**FIG. 1. Interaction of adenosine with hCNT1.** *A*, human CNT1 mRNA was injected into oocytes, and 3 days later uptake of 50  $\mu\text{M}$  [ $^3\text{H}$ ]uridine (*U*) in the absence and in the presence of 2 mM adenosine (*A*) was measured. Also, uptake of 50 and 250  $\mu\text{M}$  [ $^3\text{H}$ ]adenosine was assayed. Uptake of uridine but not of adenosine was found, although adenosine inhibited uridine uptake by  $\sim 90\%$ . Data represent the mean of 8–10 measurements, and the error bars indicate the S.E. *NI*, non-injected oocytes. *B*, a hCNT1-expressing oocyte was held at  $-50$  mV and perfused with  $\text{Na}^+$  buffer in the absence of substrate (*open box*), and current was continuously recorded (base-line current). The addition of 0.5 mM uridine (*arrow* and *gray box*) induced an inward current of  $\sim 90$  nA. The oocyte was then washed out with  $\text{Na}^+$ -free buffer (*black box*), which blocked the uridine inward current and the base-line current and with  $\text{Na}^+$  buffer until the current returned to base line. The addition of 1 mM adenosine does not induce any inward current, indicating that it is not transported. *C*, the membrane potential of a hCNT1-expressing oocyte was clamped at  $-50$  mV, and concentration-dependent inhibition by adenosine of the uridine-induced current was recorded. The plot represents the uridine (0.25 mM)-induced current inhibited against the adenosine concentration (25, 50, 500, 1000, and 2500  $\mu\text{M}$ ). An  $\text{IC}_{50}$  of

10 mM HEPES-Tris, pH 7.5) containing [ $^3\text{H}$ ]uridine (specific activity, 36.0 Ci/mmol; PerkinElmer Life Sciences) or [ $^3\text{H}$ ]adenosine (specific activity 23.0 Ci/mmol; Sigma) at the indicated concentrations. Inhibition of uridine uptake by adenosine was measured by adding the non-radiolabeled adenosine (2 mM) to the uptake solution containing the radiolabeled uridine (50  $\mu\text{M}$ ). After the incubation period had elapsed, the  $^3\text{H}$  content of each oocyte was determined by liquid scintillation counting. Uptakes are expressed as pmol/oocyte h.

**Electrophysiology**—The electrophysiology experiments were performed using the two-microelectrode voltage clamp method (13, 15, 16). The oocyte membrane potential was normally held at a holding potential ( $V_h$ ) of  $-50$  mV, and continuous current data were recorded using Axoscope V1.1.1.14 (Axon Instruments, Foster City, CA). To obtain current/voltage relationship, 11 pulses of potential (test potential) between  $+50$  and  $-150$  mV ( $-20$ -mV decrement) were applied for 100 ms using pClamp 6 software (Axon Instruments, Foster City, CA). The jump from the holding potential to the test potential generates the “on” current, and the return from the test potential to the holding potential, before the next jump, generates the “off” current.

**Steady-state Kinetics**—The apparent affinity constant ( $K_{0.5}^S$ ) and the maximal current ( $I_{\text{max}}^S$ ) for saturating nucleoside concentrations were obtained by fitting the steady-state currents (*I*) at each membrane potential to the equation,

$$I = I_{\text{max}}^S [S]^n / (K_{0.5}^S)^n + [S]^n \quad (\text{Eq. 1})$$

where [*S*] is the nucleoside concentration (seven concentrations, from 2  $\mu\text{M}$  to 1 or 5 mM, depending on the nucleoside), and *n* is the Hill coefficient, which for nucleoside kinetic analysis is 1. The fit was performed using the non-linear fitting method in SigmaPlot 8 (SPSS, Chicago, IL). Uridine, cytidine, thymidine, adenosine, and 5'-DFUR were purchased from Sigma, and gemcitabine was from University Hospital (University of Navarra, Pamplona, Spain).

For  $\text{Na}^+$  activation experiments saturating concentrations of uridine (0.25 or 0.5 mM) were applied as  $\text{NaCl}$  concentration was varied between 0 and 100 mM (0.25, 0.5, 1, 2, 4, 5, 20, and 100 mM), substituting choline for  $\text{Na}^+$ . Uridine-dependent currents at each voltage were fit to Equation 1, where in this case *I* is the uridine-induced steady-state current,  $I_{\text{max}}^S$  is maximal uridine current at saturating  $\text{Na}^+$  concentrations, [*S*] is the  $\text{Na}^+$  concentration, and  $K_{0.5}^S$  is the sodium concentration at half-maximal current.

The apparent inhibition constant,  $K_i$ , for adenosine was determined at  $-50$ -mV membrane potential by measuring uridine or thymidine (0.25 or 0.5 mM)-induced currents in the presence of different adenosine concentrations (25, 50, 100, 500, 1000, 2500  $\mu\text{M}$ ) by continuous current recording. Because uridine/thymidine steady-state currents slowly decreased with time (Figs. 1*B* and 6*A*), the perfusion of uridine/thymidine in the presence of each adenosine concentration was performed following the  $\text{Na}^+$  buffer wash out after the substrate-induced current had been recorded. The concentration of inhibitor required to block nucleoside current by 50% ( $\text{IC}_{50}$ ) was first obtained and used to calculate the  $K_i$  using the Cheng-Prusoff equation,

$$K_i = \text{IC}_{50} / (1 + [S]/K_{0.5}^S) \quad (\text{Eq. 2})$$

where  $K_{0.5}^S$  is the affinity constant for uridine or thymidine, and [*S*] the uridine or thymidine concentration.

**Presteady-state Currents**—The presteady-state transient currents observed after voltage steps are attributed to changes in the conformation of the transporter (15–17). These capacitive currents were separated from the membrane capacitance and the steady state conductances using the fitted method (16). The transporter-mediated charge at each membrane potential was then calculated by integrating the transporter-transient currents with time. In most cases, the “off” transient was analyzed. The charge-voltage (*Q/V*) relations obtained were fit to the Boltzmann equation,

$$Q - Q_{\text{hyp}} = Q_{\text{max}} [1 - \exp(z(V_t - V_{0.5})/RT)] \quad (\text{Eq. 3})$$

where  $Q_{\text{max}} = Q_{\text{dep}} - Q_{\text{hyp}}$ ,  $Q_{\text{dep}}$  and  $Q_{\text{hyp}}$  are the charge moved at depolarizing and hyperpolarizing limits respectively, *z* is the apparent valence of the transporter,  $V_t$  is the test potential,  $V_{0.5}$  is the voltage at

$73 \pm 13$   $\mu\text{M}$  was obtained and used to calculate  $K_i$  ( $9.4 \pm 1.7$   $\mu\text{M}$ ) according to Equation 2 under “Experimental Procedures.” The *dashed curve* is the predicted by Equation 2 using the indicated  $\text{IC}_{50}$ . For the three panels similar results were obtained with oocytes from three different frog donors.

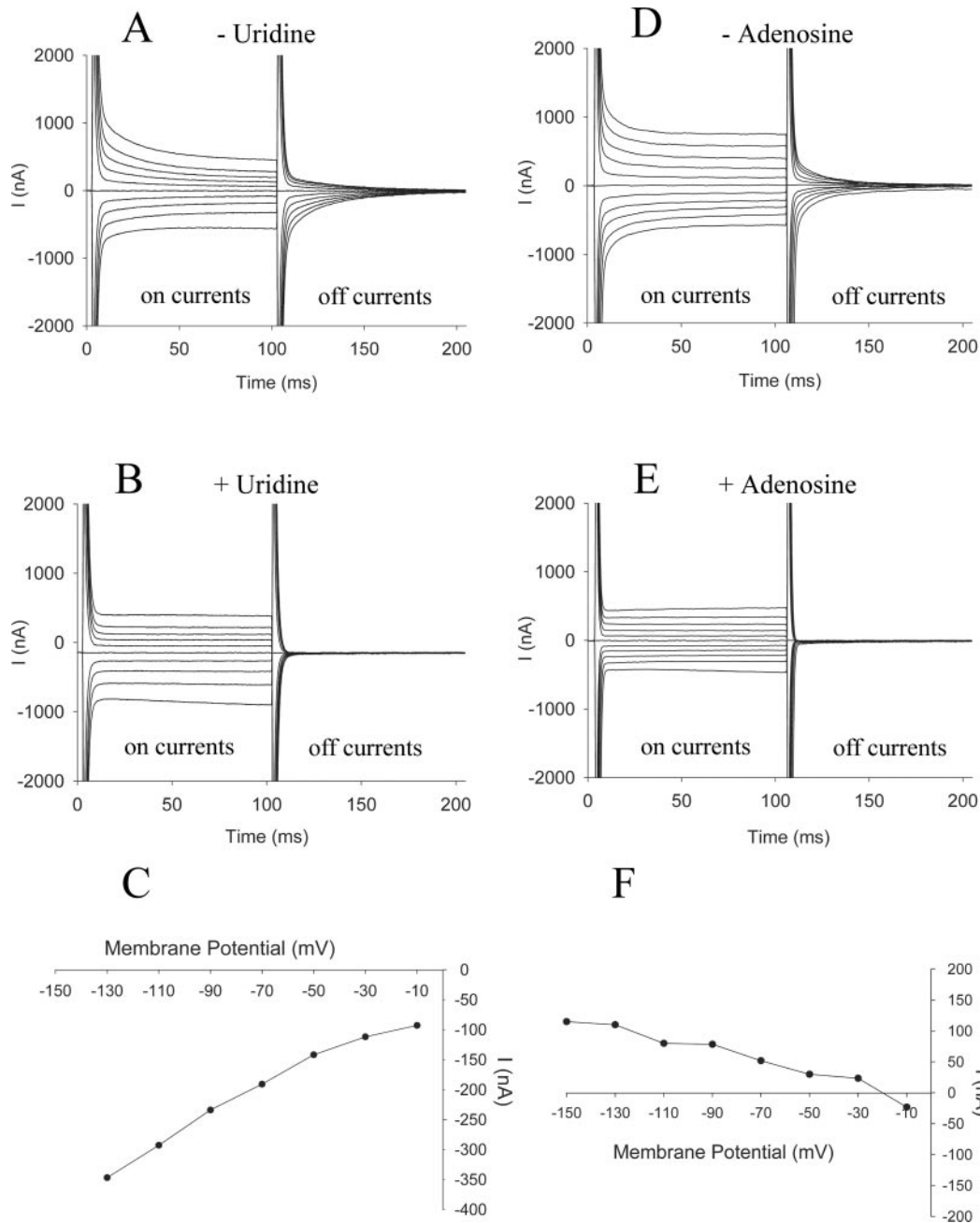


FIG. 2. **Membrane current records and steady-state currents of hCNT1 before and after the addition of nucleosides.** *A*, a hCNT1-expressing oocyte was held at  $-50$  mV and stepped to 11 test values between  $+50$  and  $-150$  mV ( $-20$ -mV decrement). In  $\text{Na}^+$  buffer and the absence of uridine the oocyte showed presteady-state currents in response to step changes in the membrane voltage and steady-state currents due to the  $\text{Na}^+$  leak through the transporter. *B*, the addition of  $10$  mM uridine blocked the presteady-state currents and caused an increase of the steady-state inward currents. *C*, steady-state current/voltage relationship induced by  $10$  mM uridine. The values were obtained as the difference between the currents obtained in the presence and the absence ( $\text{Na}^+$  leak) of uridine. *D*, a different oocyte from *A* in which presteady-state currents were also observed. *E*, these currents disappeared, and steady-state currents diminished when  $1$  mM adenosine was added. *F*, steady-state current/voltage relationship induced by  $1$  mM adenosine. Values are obtained as the difference between the currents in the presence and absence ( $\text{Na}^+$  leak) of adenosine. Adenosine decreased the  $\text{Na}^+$  leak currents, so the difference between those currents is represented as a positive outward current.

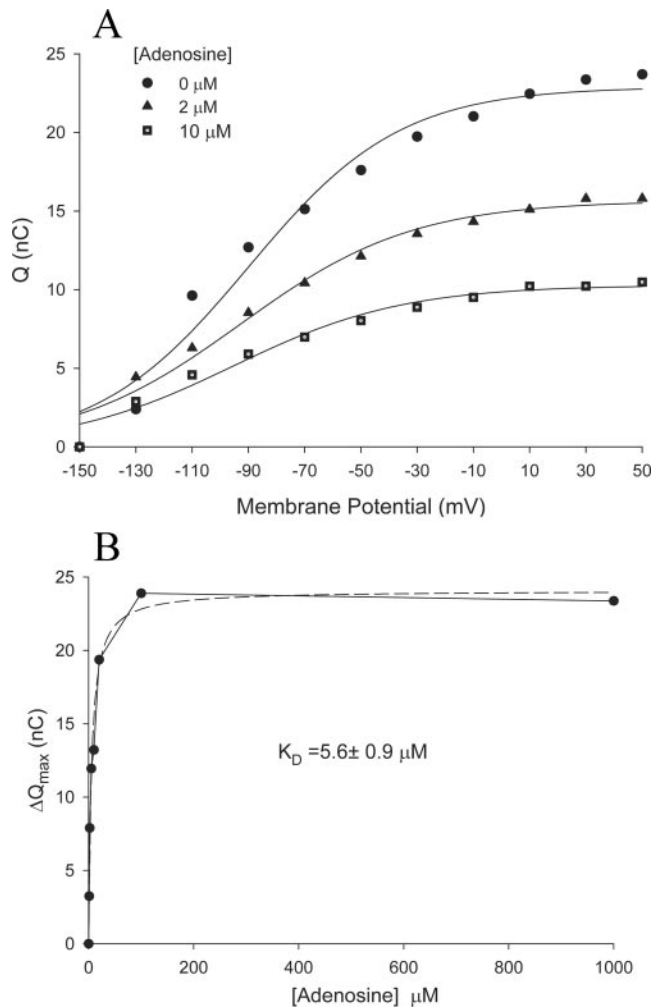
which the charge was equally distributed between depolarizing and hyperpolarizing limits,  $F$  is Faraday's constant,  $R$  is the gas constant, and  $T$  is the absolute temperature.

Charge/voltage relationship in the presence of adenosine ( $1$ ,  $2$ ,  $5$ ,  $10$ ,  $20$ ,  $100$ , and  $1000$   $\mu\text{M}$ ) was obtained for each concentration, and  $\Delta Q_{\text{max}}$  was calculated as the difference between  $Q_{\text{max}}$  in the absence and presence of adenosine.  $\Delta Q_{\text{max}}$  was plotted against adenosine concentration, and the data were fit to Equation 1 to obtain the binding constant for adenosine,  $K_D$ , where  $I$  corresponds to  $\Delta Q_{\text{max}}$  at each adenosine concentration,  $[S]$  is the adenosine concentration,  $K_{0.5}$  is the binding constant, and  $n = 1$ .

**Stoichiometry**—To determine  $\text{Na}^+$ -to-nucleoside-coupling stoichi-

ometry we directly compared unidirectional ligand uptakes ( $^{22}\text{Na}$  or  $^3\text{H}$ uridine) into voltage-clamped oocytes to the cotransporter (substrate-induced) currents over the same time course in individual cells ( $18$ – $20$ ). The nonspecific uptakes of  $^3\text{H}$ uridine and  $^{22}\text{Na}$  in non-injected oocytes were  $<1\%$  of the hCNT1-specific uptakes.

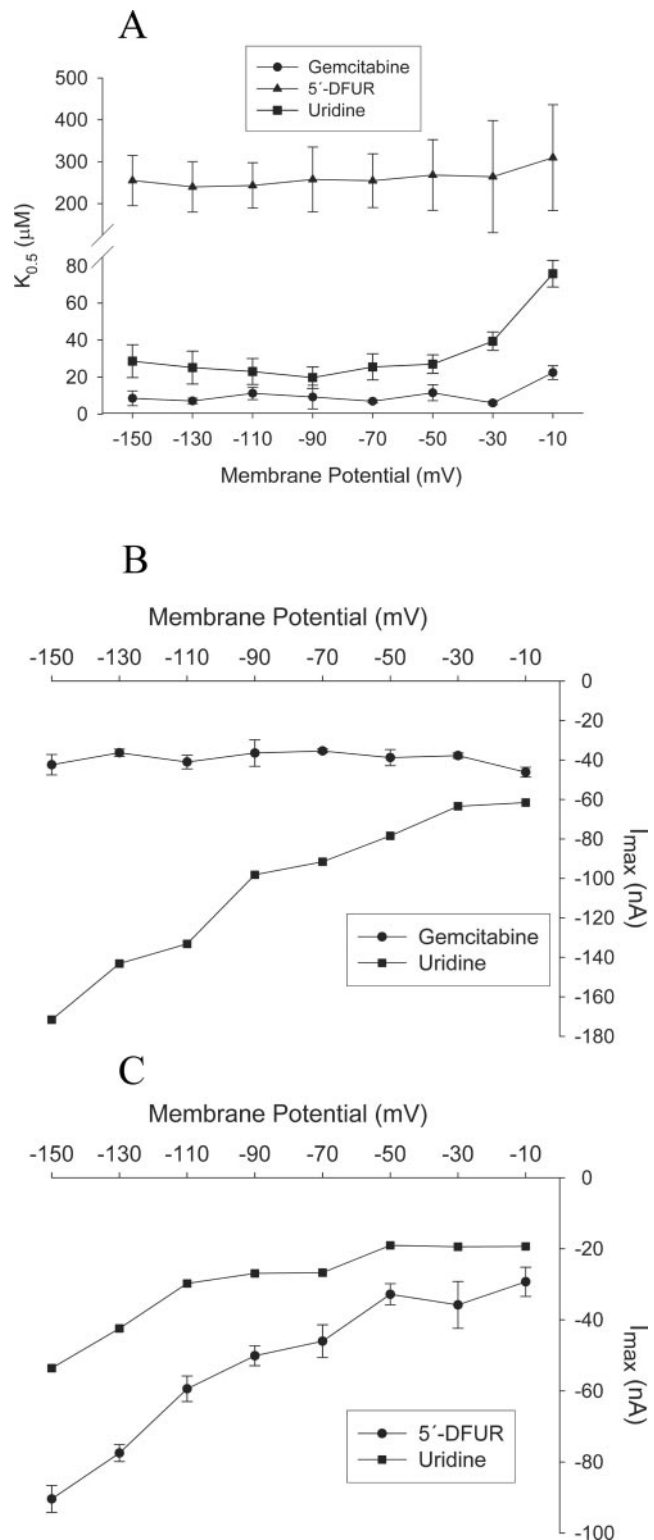
**Charge-to-nucleoside Stoichiometry**—The oocyte was voltage-clamped at  $-50$  mV and superfused with  $100$  mM  $\text{Na}^+$  medium. When the base line was stable,  $0.5$  mM  $^3\text{H}$ uridine or  $^3\text{H}$ thymidine (specific activity,  $87.0$  Ci/mmol; Amersham Biosciences) was added to the  $\text{Na}^+$  solution at a final concentration of  $1.4$  nCi/ $\mu\text{l}$ . After  $8$ – $10$  min the nucleoside was removed from the bathing solution, and the oocyte was superfused with  $\text{Na}^+$  buffer until the current returned to the base line.



**FIG. 3. Charge/voltage relationship for adenosine and kinetic analysis of  $\Delta Q_{\text{max}}$ .** *A*, the charge ( $Q$ ) moved in the presence of 0, 2, 10  $\mu\text{M}$  adenosine is plotted for each voltage. Charge was obtained by integration of the transporter presteady-state currents of an oocyte clamped at  $-50$  mV. The addition of adenosine inhibited  $Q_{\text{max}}$ . The curves are the fit to Equation 3 under "Experimental Procedures." *nC*, nanocoulombs. *B*,  $\Delta Q_{\text{max}}$  at each adenosine concentration was calculated as the difference between  $Q_{\text{max}}$  in the absence and presence of adenosine 1, 2, 5, 10, 20, 100, and 1000  $\mu\text{M}$ .  $\Delta Q_{\text{max}}$  was plotted against adenosine concentration, and the data were fit to Equation 1 to obtain the binding constant for adenosine,  $K_D$  ( $5.6 \pm 0.9 \mu\text{M}$ ). Similar results were obtained with oocytes from four different frog donors.

The oocyte was recovered from the chamber, rinsed three times in ice-cold choline buffer, and solubilized with 10% SDS for liquid scintillation counting. Uptake was expressed as pmol/oocyte. [ $^3\text{H}$ ]Uridine or [ $^3\text{H}$ ]thymidine uptake in non-injected oocytes was used to correct for endogenous uridine uptake. Nucleoside-induced current was obtained as the difference in current between base line and after the addition of nucleoside and was integrated to obtain total nucleoside-dependent charge ( $Q^{\text{nucleoside}}$ ). This charge was converted to its molar equivalent using Faraday's constant.

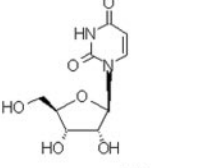
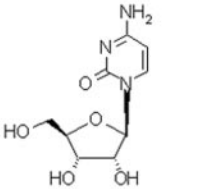
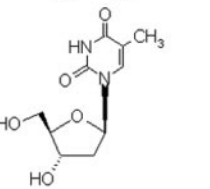
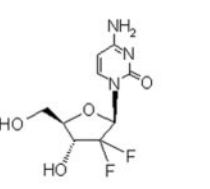
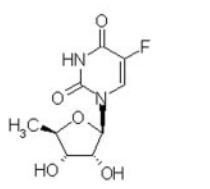
**Charge-to- $\text{Na}^+$  Stoichiometry**—Uptake of  $^{22}\text{Na}$  was optimized for specific activity and transport rate by using a saturating concentration of uridine (0.5 mM) and a  $^{22}\text{Na}$  concentration of 1 mM, close to the  $K_{0.5}^{\text{Na}^+}$ . The oocyte was clamped at  $-90$  mV and superfused with 1 mM  $\text{Na}^+$  medium. A stable base-line current was recorded, and then the bath solution was changed to 0.5 mM uridine with 1 mM  $^{22}\text{Na}$  (PerkinElmer Life Sciences) medium at a final concentration of 1.4 nCi/ $\mu\text{l}$ . After 6–10 min the solution was changed back to the  $\text{Na}^+$  medium until the current returned to base line. The oocyte was washed and solubilized as described above. The charge associated with the  $^{22}\text{Na}$  uptake induced by uridine was the difference between base-line and uridine current, whereas  $^{22}\text{Na}$  was present. Net charge transported into the oocyte was obtained by integrating the inward current produced by the nucleoside uptake in the oocyte. Charge was converted to its molar



**FIG. 4. Voltage dependence of  $K_{0.5}$  and  $I_{\text{max}}$  for uridine, gemcitabine, and 5'-DFUR.** For each nucleoside,  $K_{0.5}$  and  $I_{\text{max}}$  were obtained at every membrane potential by fitting the steady-state currents obtained at seven different concentrations (2–5000  $\mu\text{M}$ ) to Equation 1. *A*,  $K_{0.5}/V$  curves. For the three nucleosides  $K_{0.5}$  was voltage-independent and lower for gemcitabine followed by uridine and 5'-DFUR. The error bars correspond to the error of the mean from at least three determinations. *B* and *C*,  $I_{\text{max}}/V$  curves obtained in two different oocytes. Uridine curve correspond to the inward current at saturating uridine concentrations (0.5 mM), which is equivalent to the  $I_{\text{max}}$ . *B*, maximal current for gemcitabine is voltage-independent and smaller than that for uridine. *C*,  $I_{\text{max}}$  for 5'-DFUR is voltage-dependent and higher than that for uridine at all membrane potential. Similar results were obtained with oocytes from at least three different batches.

TABLE I  
Structures and apparent affinity constant for natural substrates and drugs

$K_{0.5}$  values for natural nucleosides and drugs were calculated at  $-50$ -mV membrane potentials by fitting the currents generated by the substrate at 7 concentrations ( $2 \mu\text{M}$ – $5 \text{mM}$ ) to Equation 1 under "Experimental Procedures." Currents induced by saturating nucleoside concentrations ( $I_{\text{max}}$ ) are expressed as the percentage of the current generated by saturating uridine concentrations ( $0.5 \text{mM}$ ). Values are the mean  $\pm$  S.D. of the different determinations indicated between parentheses.

$V_h = -50 \text{ mV}$		$K_{0.5} (\mu\text{M})$	% $0.5 \text{ mM}$ uridine current
	Uridine	$37 \pm 7$ (8)	100
	Cytidine	$29 \pm 8$ (6)	$47 \pm 7$ (6)
	Thymidine	$26 \pm 7$ (4)	$109 \pm 19$ (4)
	Gemcitabine	$18 \pm 5$ (8)	$33 \pm 5$ (8)
	5'-DFUR	$245 \pm 39$ (7)	$147 \pm 18$ (7)

equivalent by using Faraday's constant.  $^{22}\text{Na}$  uptake in non-injected oocytes was used to correct for endogenous  $^{22}\text{Na}$  uptake.

## RESULTS

**Interaction of Adenosine with hCNT1**—Adenosine is a purine nucleoside that had been described as a substrate of the pyrimidine-preferring nucleoside transport system later identified as CNT1. Nevertheless, discrepancy on the published data and our preliminary results prompted us to investigate whether adenosine was transported by hCNT1. Fig. 1A shows uptake of  $50 \mu\text{M}$  [ $^3\text{H}$ ]uridine by oocytes expressing hCNT1 ( $187 \pm 16 \text{ pmol/ oocyte}\cdot\text{h}$ ), but no uptake of  $50$  or  $250 \mu\text{M}$  [ $^3\text{H}$ ]adenosine was found. However,  $2 \text{mM}$  adenosine was able to inhibit uptake of  $50 \mu\text{M}$  uridine by  $90\%$ , indicating that this nucleoside is not transported by hCNT1, but it can bind to the transporter. We further demonstrated that adenosine is not a hCNT1 substrate by electrophysiological methods. A hCNT1-expressing oocyte was clamped at  $-50 \text{mV}$  and continuously perfused with  $\text{Na}^+$  buffer inducing a base-line current that corresponds to the  $\text{Na}^+$ -leak current in the absence of substrate. (Fig. 1B). The addition of  $0.5 \text{mM}$  uridine evoked an inward current of  $\sim 90 \text{ nA}$ . This current and the base-line current disappeared when the oocyte was washed out with  $\text{Na}^+$ -free buffer. The addition of  $\text{Na}^+$  buffer returned the current to the base line. Adenosine at  $1 \text{mM}$  concentration, however, did not evoke any inward current, indicating that is not

transported. We then performed experiments to obtain the apparent inhibition constant,  $K_i$ , for adenosine. Fig. 1C shows the uridine ( $0.25 \text{mM}$ )-induced current inhibited by different adenosine concentrations as a function of those concentrations in an oocyte clamped at  $-50 \text{mV}$ . For this oocyte  $\text{IC}_{50}$  was  $73 \pm 13 \mu\text{M}$ , and  $K_i^A$ , obtained as described under "Experimental Procedures," was  $9.4 \pm 1.7 \mu\text{M}$ . The mean  $K_i^A$  of three different determinations was  $6.4 \pm 1.1 \mu\text{M}$ .

Another way to determine adenosine affinity constant for hCNT1 is from the inhibition of the presteady-state currents. These currents reflect voltage-dependent processes due to charge movements caused by  $\text{Na}^+$  binding/dissociation and conformational changes involved in the reorientation of the ligand binding sites of the cotransporter in the membrane. Fig. 2A shows the current traces recorded after step changes in the membrane voltage in an oocyte held at  $-50 \text{mV}$  and perfused with  $\text{Na}^+$  buffer in the absence of substrate. The steady-state currents at  $100 \text{ms}$  correspond to the  $\text{Na}^+$  leak currents as it has been observed in many other cation-coupled transporters. Presteady-state currents can also be observed, especially at depolarizing membrane potentials. The addition of  $10 \text{mM}$  uridine increased the steady-state inward currents and inhibited the presteady-state currents (Fig. 2B). Fig. 2C represents the steady-state currents for uridine as a function of voltage. These

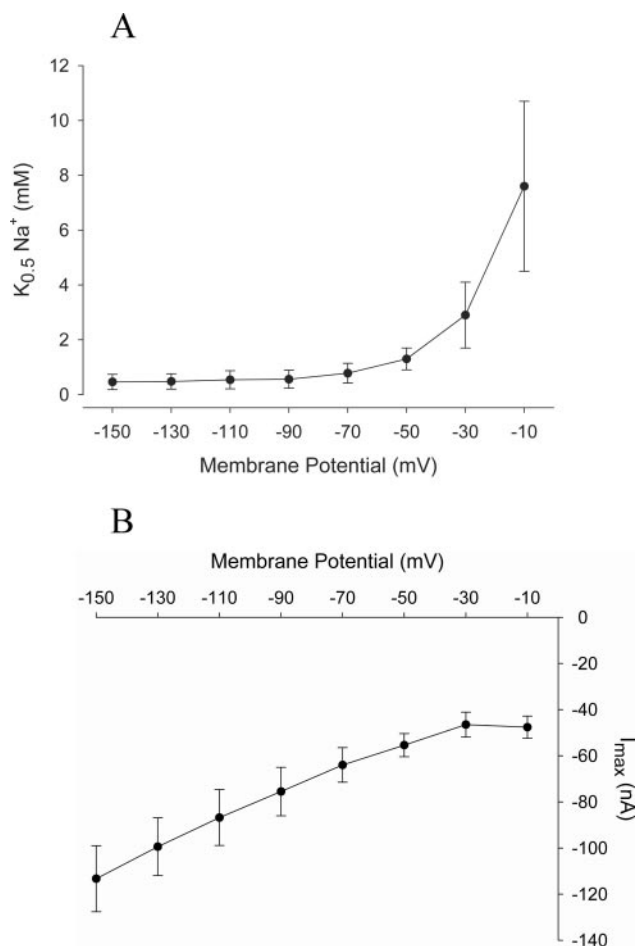


**FIG. 5.  $K_{0.5}$  and  $I_{max}$  for  $Na^+$  as a function of voltage.** The 0.25 mM uridine-induced steady-state currents were measured as a function of external  $Na^+$  concentration (0, 0.25, 0.5, 1, 2, 4, 5, 20, and 100 mM).  $K_{0.5}^{Na^+}$  and  $I_{max}^{Na^+}$  were obtained by fitting the currents at each membrane potential to Equation 1 under "Experimental Procedures."  $K_{0.5}^{Na^+}$  was voltage-independent at hyperpolarizing membrane potentials, whereas  $I_{max}^{Na^+}$  was voltage-dependent. The errors are errors of the fit. Similar results were obtained with oocytes from three different batches.

currents were obtained as the difference between the currents registered in the presence and absence of the nucleoside and increased as the membrane potential was more negative. Fig. 2, *D* and *E*, also show, in a different oocyte, the current traces recorded in the absence (Fig. 2*D*) and presence of 1 mM adenosine (Fig. 2*E*). As uridine, adenosine inhibited the presteady-state currents; however, unlike uridine, adenosine did not induce inward currents (see also Fig. 1*B*) but inhibited the  $Na^+$ -leak current. This is shown as positive currents obtained as the difference between the steady-state currents in the presence and absence of adenosine, which increased at hyperpolarizing membrane potentials (Fig. 2*F*). Notice that in Fig. 1*B* adenosine does not inhibit the  $Na^+$ -leak current due to a lower expression level of the transporter in that oocyte compared with the oocyte in Fig. 2*F*.

Charge movement as a function of membrane potential was obtained by the integration of the presteady-state current records in the absence and presence of adenosine 1, 2, 5, 10, 100, and 1000  $\mu$ M. The  $Q_{max}$  in the absence of adenosine was  $\sim$ 24 nanocoulombs and decreased with adenosine concentration to  $\sim$ 16, 11, and 5 nanocoulombs in the presence of 2, 10, and 20  $\mu$ M uridine, respectively (Fig. 3*A*).  $V_{0.5}$ , however, did not change with increasing concentrations of adenosine:  $-90 \pm 5$  mV in the absence of nucleoside and  $-93 \pm 5$ ,  $-95 \pm 5$ , and

$-114 \pm 5$  mV in the presence of 2, 10, and 20  $\mu$ M adenosine respectively. Fitting the  $\Delta Q_{max}$  data to adenosine concentration (Fig. 3*B*) indicated a binding constant,  $K_D^A$ , of  $5.6 \pm 0.9$   $\mu$ M (mean of four determinations,  $6.5 \pm 1$   $\mu$ M), a value close to the  $K_i^A$  previously obtained. All these results indicated that adenosine is not a substrate of hCNT1 but is a high affinity blocker able to inhibit uridine-induced inward currents, the  $Na^+$ -leak currents, and the presteady-state currents observed in hCNT1.

**Kinetic Parameters for Nucleosides and  $Na^+$  as a Function of Membrane Potential**—We have previously demonstrated that the drugs gemcitabine and 5'-DFUR are substrates of hCNT1. In the present work we studied the influence of the membrane potential on the kinetic parameters for the two nucleoside derivatives. Fig. 4*A* shows the  $K_{0.5}^S/V$  relationship for the two drugs and uridine.  $K_{0.5}^S$  is voltage-independent at hyperpolarizing membrane potentials for the three nucleosides, for gemcitabine, around half that for uridine, and for 5'-DFUR, one order of magnitude higher. At  $-50$  mV  $K_{0.5}^S$  values were  $11 \pm 4$ ,  $27 \pm 5$ , and  $268 \pm 84$   $\mu$ M for gemcitabine, uridine, and 5'-DFUR, respectively (Fig. 4*A*).  $I_{max}$  was voltage-dependent for uridine (Fig. 4, *B* and *C*) and thymidine (data not shown) but was voltage-independent for gemcitabine (Fig. 4*B*) and cytidine (data not shown). Maximal current for gemcitabine was 49 and 25% that for uridine at  $-50$  and  $-150$  mV, respectively (Fig. 4*B*), and  $I_{max}$  for 5'-DFUR was  $\sim$ 170% that for uridine at all membrane potentials (Fig. 4*C*).

Table I summarizes the  $K_{0.5}$  values and maximal currents in percentage of uridine current at saturating concentrations for the three natural substrates of hCNT1 and the two nucleoside-derived drugs at  $-50$  mV of membrane potential. The three natural nucleosides uridine, cytidine, and thymidine show the same affinity. However, cytidine induces half of the uridine and thymidine maximal currents. Gemcitabine, a cytidine-derived drug, shows a decrease in both  $K_{0.5}$  (2-fold) and  $I_{max}$  (2.5-fold) compared with uridine. The other nucleoside, 5'-DFUR, is a uridine-derived capecitabine metabolite that shows a higher affinity constant (one order of magnitude) and maximal current (1.5-fold) than uridine.

Electrophysiological experiments performed to determine whether  $H^+$ ,  $K^+$ , or  $Cl^-$  are involved in the nucleoside transport and contribute to generate the current revealed that none of them altered the nucleoside-induced current (data not shown). Therefore,  $Na^+$  is the only ion coupled to nucleoside transport. The kinetic parameters of  $Na^+$  as a function of voltage were also obtained.  $K_{0.5}^{Na^+}$  was voltage-independent at hyperpolarized membrane potentials (Fig. 5*A*),  $1.3 \pm 0.4$  and  $0.46 \pm 0.28$  mM at  $-50$  and  $-150$  mV, respectively.  $I_{max}^{Na^+}$  was voltage-dependent (Fig. 5*B*),  $-55 \pm 5$  and  $-113 \pm 14$  nA at  $-50$  and  $-150$  mV, respectively. The apparent affinity constant for  $Na^+$  obtained as the mean from four different determination was  $1.2 \pm 0.2$  mM at  $-50$  mV membrane potential.

**hCNT1 Stoichiometry**—To determine charge/nucleoside stoichiometry we measured nucleoside-induced current and [ $^3H$ ]uridine or  $^{22}Na$  uptake in the same hCNT1-expressing oocyte over the equal time course. Fig. 6*A* shows an example of an oocyte clamped at  $-50$  mV and superfused with 100 mM  $Na^+$  buffer, which produced the base-line current due to the  $Na^+$  leak. The addition of 0.5 mM [ $^3H$ ]uridine induced an inward current of  $\sim$ 175 nA. When the nucleoside was removed from the bath the current returned to the base line. The current was integrated with time to determine the nucleoside-dependent net charge influx ( $Q^{nucleoside}$ ) that was  $8.4 \times 10^{-5}$  coulombs of positive charge. This charge was converted to its molar equivalent, 0.87 nmol, and compared with the nucleoside [ $^3H$ ]uridine uptake, 0.48 nmol, resulting in a charge-to-nucleoside ratio of 1.81:1 for this oocyte. The same process was repeated with 21

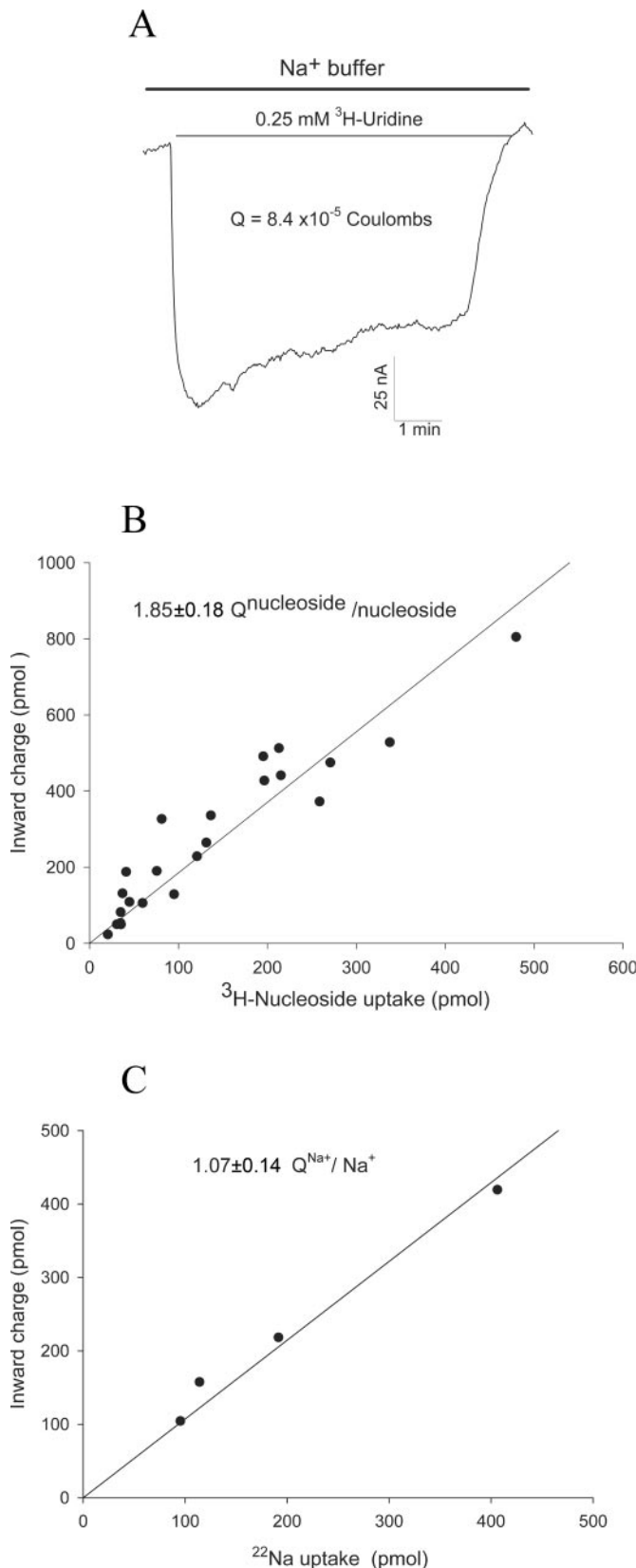


**FIG. 6. Charge-to-nucleoside and charge-to-Na<sup>+</sup> stoichiometry for hCNT1.** *A*, a representative experiment showing [<sup>3</sup>H]uridine-induced inward current in an hCNT1-expressing oocyte. Membrane potential was held at -50 mV, and oocyte perfused with Na<sup>+</sup> buffer and a stable base-line current were recorded. The addition of 0.25 mM uridine increased the inward current to ~175 nA. After 8 min uridine was removed from the bath by perfusing uridine-free Na<sup>+</sup> buffer, and the current returned to base line. The transported charge, *Q*, was calculated as the integral of the nucleoside-dependent current over 8

oocytes and [<sup>3</sup>H]uridine or [<sup>3</sup>H]thymidine concentrations of 0.5 or 0.25 mM. All the data were fitted to a single regression line. For all oocytes tested, the value of  $Q^{\text{nucleoside}}/\text{nucleoside uptake}$  was  $1.85 \pm 0.18$  (Fig. 6*B*), indicating that two net inward positive charges were transported for every nucleoside cotransported.

Similar to the former experiments, the relationship between charge influx and <sup>22</sup>Na uptake was measured in 4 oocytes clamped at -90 mV. The oocytes were superfused with 1 mM Na<sup>+</sup> solution, and after stable base line, 0.5 mM uridine with 1 mM <sup>22</sup>Na was added. The uridine-dependent inward current was recorded, and <sup>22</sup>Na uptake was measured in the same oocyte. Net charge transported ( $Q^{\text{Na}^+}$ ) was plotted against the radiolabeled <sup>22</sup>Na uptake, and data were fitted to a regression line with a slope of  $1.07 \pm 0.14$  (Fig. 6*C*), indicating that 1 net inward positive charge was transported for every Na<sup>+</sup> ion cotransported.

#### DISCUSSION

The two-electrode voltage clamp technique allows investigation of the mechanism of membrane transporters and isolates partial reactions of the transport cycle to determine the mode of action of substrates and inhibitors. We previously reported that hCNT1 is electrogenic and transports gemcitabine and 5'-DFUR, an intermediate metabolite of capecitabine and immediate precursor of the active drug 5-fluorouracil (6, 7). Nevertheless a complete electrophysiological characterization of the basic properties of hCNT1-mediated translocation has not been performed yet, and more surprisingly, the exact role of adenosine in hCNT1 function has not been addressed either.

*Interaction of Adenosine with hCNT1*—Adenosine had been described as a poor substrate of the pyrimidine-preferring CNT1 transport system. In oocytes expressing rCNT1 and measuring [<sup>3</sup>H]adenosine fluxes it was found that adenosine was transported with a  $K_{0.5}$  of 26 μM, close to the  $K_{0.5}$  for uridine; however,  $V_{\text{max}}$  was 200-fold lower than that for uridine (21). In COS-1 cells transfected with rCNT1 other authors obtained a  $K_{0.5}$  for adenosine of 15 μM and a  $V_{\text{max}}$  65-fold lower than that for uridine (22). Also in oocytes expressing both human and rat CNT1 it was reported that adenosine is transported, but the work showed a very small uptake of 10 μM adenosine (0.5 pmol/oocyte/10 min) and a  $K_i$  of adenosine of  $50 \pm 11$  μM (23). The present results using radiotracer uptake method and electrophysiological techniques demonstrate that adenosine is not a substrate of hCNT1 but a good inhibitor with an apparent affinity ~6-fold higher than for uridine ( $K_i^A = 6.4 \pm 1$  versus  $K_{0.5}^U = 37 \pm 7$ ). Similarly, in oocytes expressing rat CNT1 it was shown that adenosine did not induce any inward current but abolished uridine-induced current (9).

Presteady-state currents have been found in several cotransporters families, indicating that the origin of these transient currents may be similar between them (17, 24–26). Oocytes expressing hCNT1 also exhibit presteady-state currents after

min and was  $8.4 \times 10^{-5}$  C. The [<sup>3</sup>H]uridine uptake in this oocyte was 0.45 nmol after subtraction of [<sup>3</sup>H]uridine uptake over the same period in non-injected oocytes. *B*, charge-to-nucleoside stoichiometry of hCNT1. Uptake of 0.25 mM [<sup>3</sup>H]uridine or [<sup>3</sup>H]thymidine in the presence of 100 mM Na<sup>+</sup> was measured for 5–10 min as indicated in *A*. The membrane potential was held at -50 mV. The nucleoside dependent charge ( $Q^{\text{nucleoside}}$ ) was plotted against the uptake of the nucleoside. Each point corresponds to one oocyte after subtraction of the non-injected oocyte uptake. The data were fit to a linear regression with a slope of  $1.85 \pm 0.18$  charges/nucleoside. *C*, charge-to-Na<sup>+</sup> stoichiometry of hCNT1. The uridine-dependent charge and <sup>22</sup>Na uptake were simultaneously determined at -90 mV membrane potential in different hCNT1-expressing oocytes. The uridine concentration was 0.5 mM, and the Na<sup>+</sup> concentration 1 mM. The data were fit to a linear regression with a slope of  $1.07 \pm 0.14$  charges/Na<sup>+</sup>.

step changes in membrane voltage in the presence of Na<sup>+</sup> and the absence of nucleoside with comparable properties. These currents reveal voltage-dependent processes due to charge transfer caused by binding and dissociation of Na<sup>+</sup> and the conformational changes involved in the reorientation of the ligand binding sites of the cotransporter in the membrane (15–17). They decrease upon the addition of the substrate uridine or the inhibitor adenosine, as it occurs in others cotransporters (15, 20, 26, 27). This decrease on the presteady-state currents, which depends on the substrate/inhibitor concentration, indicates a reduction on charge movement (and, therefore, the number of functional transporters or  $Q_{\max}$ ) with a potency comparable with their apparent  $K_{0.5}/K_i$  (14, 16, 27, 28). Accordingly, the apparent inhibition constant for adenosine obtained by directly measuring the inhibition of uridine/thymidine-induced inward currents and measuring inhibition of the charge movement of the transporter were similar. Another characteristic of high affinity inhibitors, which is fulfilled by adenosine, is that they reduce the number of functional transporters as their concentration increases, without affecting  $V_{0.5}$  (17, 28).

**Kinetic Parameters for Nucleosides and Na<sup>+</sup> as a Function of Membrane Potential**—Using flux measurements in oocytes expressing hCNT1  $K_{0.5}$  values for 45  $\mu\text{M}$  for uridine and 24  $\mu\text{M}$  for gemcitabine and a  $V_{\max}$  for gemcitabine of 45% that for uridine (8) were reported. These results are in accordance to those obtained in the present work. Cytidine and its derivative gemcitabine induce lower  $I_{\max}$  than uridine, but cytidine shows the same  $K_{0.5}$  than uridine, whereas gemcitabine has higher affinity. On the other hand, 5'-DFUR, a uridine derivative, shows higher  $I_{\max}$  and  $K_{0.5}$  than uridine. Likewise, studies performed using SGLT1 demonstrated that phenylglucosides induce different maximal currents and show different affinities than the natural substrates. The difference in the maximal currents of those compounds is explained by a variation in the translocation rate of the sugar-Na<sup>+</sup>-loaded transporter due to their structure (14, 29). In rCNT1 it has been found that in the azacytidine molecule the change of the nitrogen from the 5 to 6-position alters the conformation of the nucleoside and dramatically decreases its transport rate (9). Similarly, the differences between the kinetic parameters of the nucleosides in the present work can be related to their structure. The lack of transportability of adenosine by hCNT1 and data obtained when analyzing its rat ortholog, showing extremely low  $V_{\max}$  values, support the view that adenosine is not a substrate for CNT1 in humans and may not be a physiological substrate in rodents. Selectivity for pyrimidines appears to be determined by a reduced number of amino acid residues in transmembrane domains 7 and 8. Ser-319, Gln-320, Ser-353, and Leu-354, when replaced by the equivalent amino acids of the purine preferring nucleoside transporter CNT2, result in a switch of selectivity from pyrimidines into purines (30). Although the contribution of other residues in nucleoside selectivity cannot be ruled out, the analysis of the primary structure of both orthologs, human and rat CNT1, reveal that sequences are identical particularly in these two transmembrane domains. A high sequence identity would argue against significant differences in substrate selectivity among orthologs. Cytidine and gemcitabine, which show lower  $I_{\max}$ , present an NH<sub>2</sub> group in the 4 position of the pyrimidine ring, whereas the other three nucleosides have an O in that position. Furthermore, gemcitabine presents two F residues in the 2' position that may contribute to the increase in affinity. In the case of 5'-DFUR, the lack of an OH group in the fifth carbon of the ribose ring and the presence of an F residue in the 5 position of the pyrimidine ring could explain the changes in its kinetic parameters.

In rabbit SGLT1 it has been demonstrated that the rate-limiting step for sugar transport is the empty carrier translocation from the internal to the external face of the membrane and that the only steps in the transport cycle considered voltage-dependent are the empty carrier translocation and the Na<sup>+</sup> binding/dissociation. As the membrane potential is made more negative, the empty carrier moves faster to the extracellular face of the membrane, more current is recorded, and the internal dissociation of Na<sup>+</sup> becomes the rate-limiting step. This mechanism explains the voltage dependence of the sugar-induced current in SGLT1 (15, 31). For the case of the transport of helicin, a glucoside derivative whose  $I_{\max}$  is voltage-independent, it was found that the constant rate of the fully loaded sugar-Na<sup>+</sup>-carrier complex from the outward to the inward facing conformation decreases and becomes the rate-limiting step of the transport cycle (14). Considering the similarity between the electrogenic properties of SGLT1 and hCNT1, we propose that the voltage independence of  $I_{\max}$  for gemcitabine and cytidine here found could also be explained as a decrease of the constant rate of the fully loaded nucleoside-Na<sup>+</sup>-carrier complex due to the structure differences between these two nucleosides and uridine, thymidine, and 5'-DFUR.

**hCNT1 Stoichiometry**—Stoichiometry for hCNT1 has been reported to be 1 nucleoside:1 Na<sup>+</sup> based on the Hill coefficient analysis (1). The Hill coefficient is often used as an indirect method to estimate the number of ligand molecules that are required to bind to a transporter to generate transport. However, for a transporter with more than one ligand binding site, the Hill equation does not reflect a physically possible reaction scheme. Only when the affinity of binding for the first ligand molecule is much lower than for the subsequent ligand molecules the Hill coefficient is an accurate estimate (32). In the present work we have directly determined the relationship between the currents and the nucleoside and Na<sup>+</sup> uptake by hCNT1. The results indicate that 2 inward charges are introduced for each nucleoside that is transported and that 1 inward positive charge is transported for each Na<sup>+</sup> ion that is cotransported with the nucleoside. Therefore, the Na<sup>+</sup>/nucleoside ratio suggests a stoichiometry of 2:1 and not of 1:1.

Finally, the unequivocal evidence that adenosine is a high affinity blocker of CNT1 raises the question of whether this purine nucleoside may exert additional physiological roles besides its known interaction with purinergic receptors. In intestinal and renal epithelia CNT1 and CNT2 are located at the apical absorptive side. CNT2 is indeed the high affinity concentrative nucleoside transporter for adenosine, and thus, CNT2 function may in practice modulate extracellular adenosine concentrations, which in turn may also determine CNT1 translocation activity. Whether this functional cross-talk really occurs in physiological models and how this may affect drug bioavailability requires further analysis.

**Acknowledgments**—We thank A. Redín for technical assistance and Dr. E. M. Wright and Dr. B. A. Hirayama for the facilities to perform the charge-to-Na<sup>+</sup> stoichiometry studies.

#### REFERENCES

1. Griffith, D. A., and Jarvis, S. M. (1996) *Biochim. Biophys. Acta* **1286**, 153–181
2. Pastor-Anglada, M., Felipe, A., and Casado, F. J. (1998) *Trends. Pharmacol. Sci.* **19**, 424–430
3. Baldwin, S. A., Mackey, J. R., Cass, C. E., and Young, J. D. (1999) *Mol. Med. Today* **5**, 216–224
4. Casado, F. J., Lostao, M. P., Aymerich, I., Larrayoz, I. M., Duflo, S., Rodriguez-Mulero, S., and Pastor-Anglada, M. (2002) *J. Physiol. Biochem.* **58**, 207–216
5. Ritzel, M. W., Ng, A. M., Yao, S. Y., Graham, K., Loewen, S. K., Smith, K. M., Ritzel, R. G., Mowles, D. A., Carpenter, P., Chen, X. Z., Karpinski, E., Hyde, R. J., Baldwin, S. A., Cass, C. E., and Young, J. D. (2001) *J. Biol. Chem.* **276**, 2914–2927
6. Lostao, M. P., Mata, J. F., Larrayoz, I. M., Inzillo, S. M., Casado, F. J., and Pastor-Anglada, M. (2000) *FEBS Lett.* **481**, 137–140
7. Mata, J. F., Garcia-Manteiga, J. M., Lostao, M. P., Fernandez-Veledo, S.,



- Guillen-Gomez, E., Larrayoz, I. M., Lloberas, J., Casado, F. J., and Pastor-Anglada, M. (2001) *Mol. Pharmacol.* **59**, 1542–1548
8. Mackey, J. R., Yao, S. Y., Smith, K. M., Karpinski, E., Baldwin, S. A., Cass, C. E., and Young, J. D. (1999) *J. Natl. Cancer Inst.* **91**, 1876–1881
9. Dresser, M. J., Gerstin, K. M., Gray, A. T., Loo, D. D. F., and Giacomini, K. M. (2000) *Drug Metab. Dispos.* **28**, 1135–1140
10. Gerstin, K. M., Dresser, M. J., and Giacomini, K. M. (2002) *Am. J. Physiol. Renal Physiol.* **283**, 344–349
11. Yao, S. Y., Ng, A. M., Loewen, S. K., Cass, C. E., Baldwin, S. A., and Young, J. D. (2002) *Am. J. Physiol. Cell Physiol.* **283**, 155–168
12. Loewen, S. K., Ng, A. M., Mohabir, N. N., Baldwin, S. A., Cass, C. E., and Young, J. D. (2003) *Yeast* **20**, 661–675
13. Birnir, B., Loo, D. D., and Wright, E. M. (1991) *Pfluegers Arch.* **418**, 79–85
14. Lostao, M. P., Hirayama, B. A., Loo, D. D., and Wright, E. M. (1994) *J. Membr. Biol.* **142**, 161–170
15. Parent, L., Supplisson, S., Loo, D. D., and Wright, E. M. (1992) *J. Membr. Biol.* **125**, 49–62
16. Loo, D. D., Hazama, A., Supplisson, S., Turk, E., and Wright, E. M. (1993) *Proc. Natl. Acad. Sci. U. S. A.* **90**, 5767–5771
17. Hazama, A., Loo, D. D., and Wright, E. M. (1997) *J. Membr. Biol.* **155**, 175–186
18. Mackenzie, B., Loo, D. D., and Wright, E. M. (1998) *J. Membr. Biol.* **162**, 101–106
19. Diez-Sampedro, A., Eskandari, S., Wright, E. M., and Hirayama, B. A. (2001) *Am. J. Physiol. Renal Physiol.* **280**, 278–282
20. Loo, D. D., Eskandari, S., Boorer, K. J., Sarkar, H. K., and Wright, E. M. (2000) *J. Biol. Chem.* **275**, 37414–37422
21. Yao, S. Y., Ng, A. M., Ritzel, M. W., Gati, W. P., Cass, C. E., and Young, J. D. (1996) *Mol. Pharmacol.* **50**, 1529–1535
22. Fang, X., Parkinson, F. E., Mowles, D. A., Young, J. D., and Cass, C. E. (1996) *Biochem. J.* **317**, 457–465
23. Ritzel, M. W., Yao, S. Y., Huang, M. Y., Elliott, J. F., Cass, C. E., and Young, J. D. (1997) *Am. J. Physiol.* **272**, C707–C714
24. Mackenzie, B., Schafer, M. K., Erickson, J. D., Hediger, M. A., Weihe, E., and Varoqui, H. (2003) *J. Biol. Chem.* **278**, 23720–23730
25. Forlani, G., Bossi, E., Perego, C., Giovannardi, S., and Peres, A. (2001) *Biochim. Biophys. Acta* **1538**, 172–180
26. Klamo, E. M., Drew, M. E., Landfear, S. M., and Kavanaugh, M. P. (1996) *J. Biol. Chem.* **271**, 14937–14943
27. Wadiche, J. I., Arriza, J. L., Amara, S. G., and Kavanaugh, M. P. (1995) *Neuron* **14**, 1019–1027
28. Hirayama, B. A., Diez-Sampedro, A., and Wright, E. M. (2001) *Br. J. Pharmacol.* **134**, 484–495
29. Diez-Sampedro, A., Lostao, M. P., Wright, E. M., and Hirayama, B. A. (2000) *J. Membr. Biol.* **176**, 111–117
30. Loewen, S. K., Ng, A. M., Yao, S. Y., Cass, C. E., Baldwin, S. A., and Young, J. D. (1999) *J. Biol. Chem.* **274**, 24475–24484
31. Parent, L., Supplisson, S., Loo, D. D., and Wright, E. M. (1992) *J. Membr. Biol.* **125**, 63–79
32. Weiss, J. N. (1997) *FASEB J.* **11**, 835–841